doi:10.2533/chimia.2024.304 Chimia 78 (2024) 304–312

X-ray Spectroscopy at the SuperXAS and Debye Beamlines: from *in situ* to *Operando*

Aram Bugaev, Adam H. Clark, Nina S. Genz, Olga V. Safonova, Grigory Smolentsev, and Maarten Nachtegaal*

Abstract: Understanding structure–performance relationships are essential for the rational design of new functional materials or in the further optimization of (catalytic) processes. Due to the high penetration depth of the radiation used, synchrotron-based hard X-ray techniques (with energy > 4.5 keV) allow the study of materials under realistic conditions (*in situ* and *operando*) and thus play an important role in uncovering structure-performance relationships. X-ray absorption and emission spectroscopies (XAS and XES) give insight into the electronic structure (oxidation state, spin state) and local geometric structure (type and number of nearest neighbor atoms, bond distances, disorder) up to ~5 Å around the element of interest. In this mini review, we will give an overview of the *in situ* and *operando* capabilities of the SuperXAS beamline, a facility for hard X-ray spectroscopy, through recent examples from studies of heterogeneous catalysts, electrochemical systems, and photoinduced processes. The possibilities for time-resolved experiments in the time range from ns to seconds and longer are illustrated. The extension of X-ray spectroscopy at the new Debye beamline combined with operando X-ray scattering and diffraction and further developments of time-resolved XES at SuperXAS will open new possibilities after the Swiss Light Source upgrade mid 2025.

Keywords: Catalysis · Electrochemistry · *In situ* · *Operando* · Photocatalysis · Photoinduced processes · Pump-probe · XAS · XES · EXAFS · XANES

Authors in order of appearance in front of the Swiss Light Source.

Aram Bugaev obtained his PhD in Chemistry and Materials Sciences from the University of Turin (Italy) in 2017, followed by a Habilitation Degree in Physics from the Southern Federal University (Russia) in 2021. Since 2023 he joined the *operando* group as a postdoctoral research fellow. His research is focused on the *operando* characterization of homogenous and heterogenous catalysts by means of X-ray absorption spectroscopy. Aram has conducted more than 80 experiments at leading synchrotron radiation facilities in Europe. Additionally, he specializes in the development of novel analytical approaches, including those integrating machine learning algorithms.

Adam H. Clark received his molecular modelling and materials science doctorate from University College London (UK) in 2018 with a background in applying synchrotron scattering and spectroscopy techniques. He then moved to Switzerland to take up a postdoctoral fellow position at the Paul Scherrer Institute in the *operando* spectroscopy group and subsequently as a beamline scientist at the SuperXAS beamline, working on the development of software for the processing and analysis of large time-series XAS datasets. In 2023 he joined the Debye beamline with the focus of developing a platform for combined X-ray scattering and absorption spectroscopy to investigate functional materials under operation.

Nina S. Genz studied chemistry at Technical University Berlin (Germany) and obtained her PhD with Prof. T. Ressler. She then started her postdoctoral stay at Utrecht University (Netherlands) with Prof. B. Weckhuysen and obtained a Walter Benjamin Fellowship from the German Research Foundation to focus on advanced *operando* characterization of multi-metal CO_2 hydrogenation catalysts. Here, she started specializing on X-ray based characterization techniques and went for a research stay to University of Helsinki (Finland) with Prof. S. Huotari. In 2023, she joined the Paul Scherrer Institute as a tenure-track scientist at the SuperXAS beamline. Her research focuses on *operando* characterization of function materials with a special emphasis on C1 chemistry.

Olga V. Safonova studied chemistry at the Lomonosov Moscow State University where she obtained her PhD in inorganic chemistry with Prof. A. Gaskov. She then worked as a postdoc and a staff scientist at the European Synchrotron Radiation Facility studying heterogeneous catalysts with X-ray absorption and diffraction methods. Since 2010, she has been a senior scientist at the Paul Scherrer Institute where she participates in the management of the SuperXAS beamline at the Swiss Light Source and performs her independent research funded by SNSF and EU programs focused on heterogeneous catalysis and *operando* X-ray absorption spectroscopy.

Grigory Smolentsev obtained his PhD degree in 2006 and started his research career at Rostov State University (Russia), developing theoretical methods for analysis of X-ray absorption spectra. During a postdoctoral fellowship at Lund University (Sweden) he has transitioned from theoretical to experimental

*Correspondence: Dr. M. Nachtegaal, E-mail: maarten.nachtegaal@psi.ch, PSI Forschungsstrasse 111, CH-5232 Villigen-PSI, Switzerland

work investigating molecular systems for artificial photosynthesis. In 2011 he started his career as an experimentalist at the Paul Scherrer Institute working on the development of pump-probe X-ray spectroscopic techniques first as a postdoctoral fellow at the SuperXAS beamline and since 2015 as a senior scientist. He is currently responsible for the development and operation of laser pump X-ray probe spectroscopy techniques at two SLS beamlines (SuperXAS and Phoenix).

Maarten Nachtegaal received his PhD degree in environmental chemistry at the University of Delaware (USA), with Prof. D. L. Sparks. After a postdoctoral fellow position at ETH, he joined PSI in 2005. He is currently heading the center for *operando* spectroscopy studies (COSS) at the Paul Scherrer Institute (Switzerland) and leading research groups that operate and further develop two beamlines for *operando* chemistry research at the Swiss Light Source: the SuperXAS and Debye beamlines. He has a strong interest in cross-disciplinary research and the development of new *operando* experimental methods to determine the structure of the catalytic active site.

1. Introduction

Synchrotron facilities produce brilliant X-ray beams over a wide X-ray energy range. Switzerland has its own synchrotron for applied research, the Swiss Light Source (SLS) located at the Paul Scherrer Institut (PSI), which is currently upgrading towards a diffraction-limited light source. Even more brilliant (number of photons per second per energy bandwidth per square mrad per square mm) and coherent X-rays will be available when SLS 2.0 is opened up for users in 2025.

The SuperXAS beamline at SLS, in operation since 2008, is a beamline constructed for *operando* studies of functional materials by X-ray absorption and emission spectroscopy (XAS and XES). A new sister beamline, the Debye beamline, saw its first light in the autumn of 2023, and will allow for quasi-simultaneous XAS and XRD studies on the same sample and under the same *operando* conditions. Both beamlines start at an energy of 4.5 keV, which is sufficiently high so that X-rays can penetrate through air and reaction cell window materials, allowing for *operando* studies, *i.e.* following simultaneously the evolution of structure and activity of the functional material.

XAS is inherently an element-specific technique giving access to the electronic structure (in a simple picture the oxidation state) and the local structure (coordination number, bond distance and disorder) up to *ca.* 5 Å around the element of study. In short, to collect XAS spectra, the X-ray energy is tuned around the binding energy of a core electron. When the incident energy matches or exceeds the binding energy of the core electron, an electron is excited into unoccupied and continuum states. This absorption event gives rise to a characteristic absorption edge whose position depends on how strongly the core electron is bound to the nucleus. This, in turn, depends on the potential of the nucleus and the number of outer electrons, and thus, the absorption edge position reflects the oxidation state of the metal of interest. The region around the absorption edge is called the X-ray absorption near edge structure (XANES). When the energy of the incident X-ray photon is sufficient to ionize the absorbing element under study, the resulting photoelectric wave spherically propagates and interacts with its neighboring environment, giving rise to an interference pattern manifesting as oscillations in the absorption coefficient, depending on how much kinetic energy is given to the photo-electron. This region, starting about 30 eV above the absorption edge, is called the extended X-ray absorption fine structure (EXAFS), and gives information on the chemical identity and number of nearest neighbors, bond distances and the degree of disorder. More information on the technique can be found in dedicated reviews and books, *e.g.* XAFS for Everyone.[1]

While XAS probes the electronic structure through the density of unoccupied states, the occupied states can be probed by XES which provides complementary electronic structure information. Very briefly, when the excited state with a core hole, created due to the absorption of an X-ray photon, relaxes and is filled by the transition of an electron from a higher shell, a secondary photon is released with an energy specific to the difference in electron orbital energy levels. This process gives rise to characteristic photoemission lines. The fine structure of these lines can be scanned by X-ray emission spectrometers with *ca.* 1 eV resolution, giving additional information on the occupied density of states, with sensitivity to spin state, oxidation state of transition metals as well as specific details corresponding to the nature of ligands.

XAS and XES offer various possibilities for investigating the dynamics of structural evolution of various catalytic systems. The required time resolution depends on the specific scientific question and the experimental setup. The SuperXAS and Debye beamlines at SLS enable measuring XAS spectra with sub-second repetition rates and thus allows the (electronic) structure of dynamic processes to be followed.[2] Slower processes (hour-scale) can be alternatively studied by laboratory-based XAS spectrometers if the element of interest is accessible (mainly K-edges of 3d transition metals and L-edges of 5d metals).[3,4]

In this mini-review, we will show recent examples of the application of XAS and XES to acquire insights into the structure of the catalytic active sites as well as reaction mechanisms in heterogeneous catalysis, electro-catalysis and photo-catalysis collected in the last 10 years at the SuperXAS beamline. These examples show: i) the strength and current capabilities of X-ray spectroscopy for *operando* studies; ii) state-of-the-art in *operando* reaction cell development; and iii) highlights of the recent technical developments at the SuperXAS beamline. We hope these examples inspire you to apply X-ray spectroscopy to your research, either at the SuperXAS and Debye beamlines at the SLS or the SNBL beamline (BM31) at European synchrotron radiation facility[5] (see Abdala *et al.* in this issue of *CHIMIA*) or for studying S, P, Si or Al chemistry (below 4.5 keV) at the Phoenix beamline of the SLS.

2. A Service for *Ex Situ* Sample Measurements

With the growth in user communities across a wide array of research fields spanning chemical, physical and biological sciences, the demand for rapid access to synchrotron measurements has necessitated the provision of a service for *ex situ* materials characterization under the umbrella of the MESQUICK proposal system. Prior to the SLS 2.0 upgrade, the SuperXAS beamline gave access to synchrotron XAS for mail-in samples with 49 completed proposals in the first year facilitating the answering of a wide array of research questions. *Ex situ* measurements can be highly valuable in uncovering the structure of as-prepared materials,[6] in probing the effect of synthetic steps during catalyst preparation,[7] exploring catalyst stability and deactivation mechanisms,[8] investigating capacity fading mechanisms in battery materials,[9] studying long-term aging in slow geochemical processes,[10] or investigating the metal binding sites for drug discovery[11] as pertinent recent examples.

3. Following the Dynamics of Heterogeneous Catalysts Under Steady-state and Transient Conditions

From day one of user operation at the SuperXAS beamline, XAS has been used to identify the dynamic structure of heterogeneous catalysts.[12] XAS investigations are performed under steady-state or transient conditions, depending on the specific catalytic process and scientific question to be answered. In catalysis research, the initial step, after the synthesis of the catalyst, is usually an activation step in which the catalyst's active

sites are generated. Subsequently, it is important to follow the evolution of the active sites under relevant operating conditions and, finally, to understand potential deactivation processes.

Catalyst reduction is often employed as an activation step, and therefore, temperature-programmed reduction (TPR) studies with controlled gas or liquid environments are commonly undertaken.[13–17] For example, TPR-XAS studies of a bimetallic Pt-FeO_x/Al_2O_3 catalyst identified a concomitant reduction of both Pt and Fe species starting at around 90 °C (Fig. 1a). The reduction of the Pt species proceeded from oxidic Pt over Pt-H towards metallic Pt, while reduction generated only Fe^{2+} species with a significant proportion of Fe^{3+} remaining.[18] Catalyst activation can also be investigated in liquid environments. More specifically, TPR studies were utilized to track the *in situ* reduction of alumina-supported PdO in H_2-saturated cyclohexane to quantitatively assess the formation/consumption of Pd hydrides.[17] This approach made it possible to follow the evolution of Pd hydrides and carbides during furfural hydrogenation in 2-propanol.[16] This methodology is not reaction-limited and offers a valuable approach to gain a deeper understanding of the *in situ* formation and subsequent consumption of Pd hydrides in liquid-phase hydrogenation reactions.

In addition to these synchrotron-based TPR studies, new insights into synergistic effects of multi-metal CO_2 hydrogenation catalysts (6 wt% total metal on SiO_2) can also be gained from studying the catalyst activation with laboratory-based *operando* XANES studies. While the formation of a bimetallic Ni-Fe catalyst increased the reducibility of both the Ni and Fe species, an Ni-Cu bimetallic catalyst only increased the reducibility of the Ni species leaving the oxidation state of the Cu species unaffected (Fig. 1b). In a trimetallic Ni-Fe-Cu catalyst, the reduction of all metals is facilitated. Moreover, it was possible to correlate the observed metal speciation differences from the activation with the catalytic performances of these multi-metal systems.[3]

Once the catalyst activation step is completed, the evolution of the electronic and structural properties of a catalyst under operating conditions is of particular interest. Therefore, *in situ* and *operando* XAS studies under steady-state conditions are often performed yielding valuable insight into the active catalyst structure. Where applicable, further insights into possible catalyst deactivation mechanisms can also be deduced. Such *operando* steady-state XAS studies were key in identifying the Fe^{2+} concentration in Pt-FeO_x catalysts as a descriptor for the catalyst activity in preferential CO oxidation at ambient temperature. Moreover, the observed deactivation of the catalyst with time on stream directly correlated with the decreasing concentration of Fe^{2+} due to oxidation to inactive Fe^{3+} oxides.[19]

Another example for the importance of *in situ*/*operando* XAS studies is the use of bifunctionality of single-atom catalyst (Pt, Au, Ru) supported on carbons (activated, non-activated, N-doped) in catalytic acetylene hydrochlorination. Besides investigating the influence of synthesis parameters (*e.g.* solvent, thermal activation temperature, carbon support) towards achieving stable single-atom catalysts,[8] following the *in situ* activation allowed the elucidation of the anchoring of Pt to cavities in the carbon support. Furthermore, steady-state XAS performed under varied operating

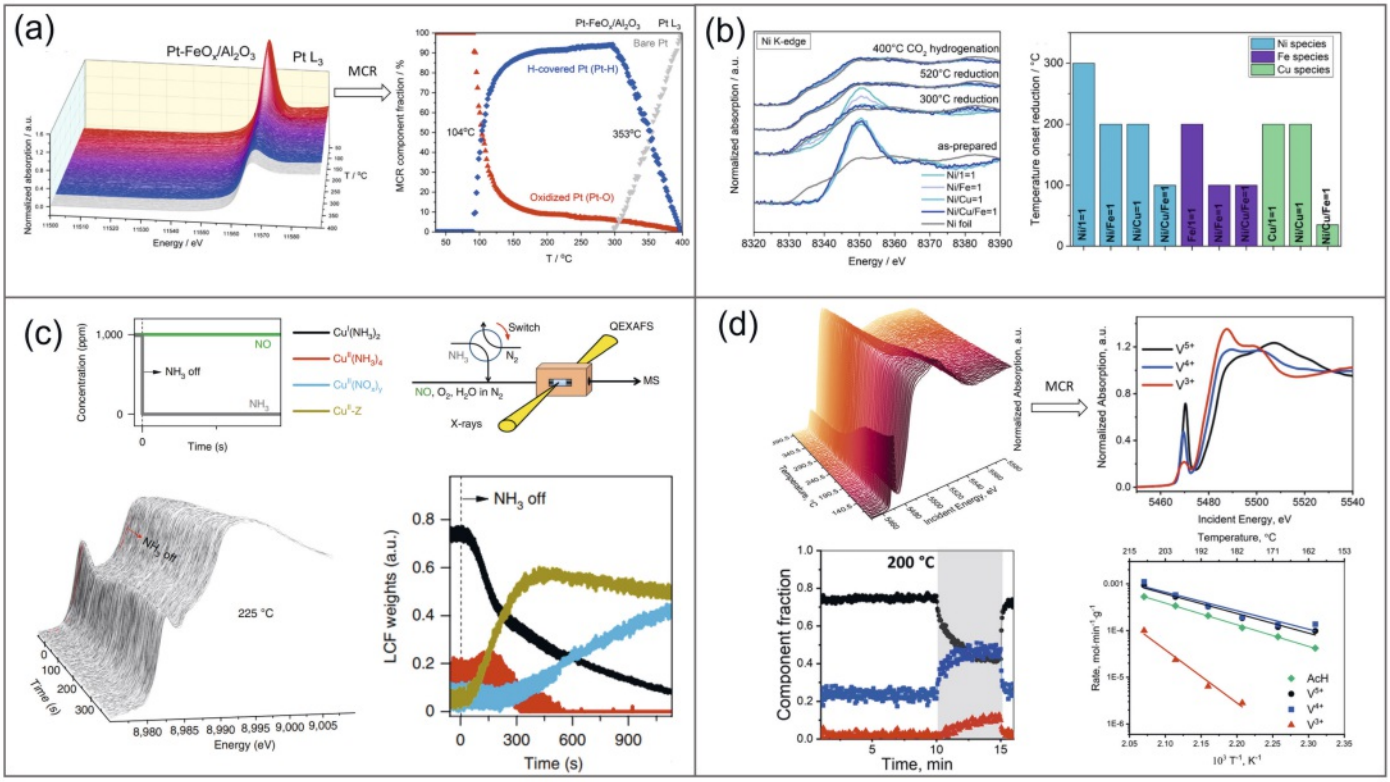

Fig. 1. a) An example of time-resolved Pt L_3-edge XANES data of a Pt-FeO_x/Al_2O_3 catalyst collected during TPR in 5% H_2 together with the percentage of the corresponding spectral components. Reproduced with permission from ref. [18]. Copyright **2021** *American Chemical Society* b) Selected *operando* Ni K-edge laboratory-based XANES data recorded during reduction and CO_2 hydrogenation for several multi-metal catalysts, and the corresponding temperatures of the reduction onset. Reproduced with permission from ref. [3] and used under CC BY 4.0 https://creativecommons.org/licenses/by/4.0/. c) The scheme of *operando* transient experiment, time-resolved XANES spectra collected at the Cu K-edge and the corresponding weights of the spectral components for Cu-SSZ-13 under relevant conditions of selective catalytic reduction of NO_x by ammonia. Reproduced with permission from ref. [24] d) Time-resolved *operando* V K-edge XANES of VO_x species in VO_x/TiO_x/SiO_2 catalyst measured during ethanol TPR; V^{5+}, V^{4+}, and V^{3+} components resolved with multivariate curve resolution analysis (MCR); the corresponding concentration trends during oxygen cut-off at 200 °C and derived Arrhenius plot. Adapted with permission from ref. [25] and used under CC BY 4.0 https://creativecommons.org/licenses/by/4.0/.

conditions allowed the deduction that the activation of hydrogen chloride is exclusively associated to the metal atoms while their coordination with the carbon supports is crucially determined by the activation step and functionality of the support. Moreover, with complementary information from EPR, the neighboring sites in the support were identified as acetylene absorption sites and were responsible for the catalyst deactivation by coking. This study demonstrated that both the metal sites and the carbon support should be designed in a concerted approach to enhance the catalytic activity through optimizing the hydrogen chloride and acetylene interactions.[14]

Circumventing catalyst deactivation also plays a crucial role in the rational design of next-generation catalysts; dry reforming of methane (CH_4) constitutes a significant challenge in this regard. *In situ* and *operando* XAS studies can provide valuable insight, as shown by an example of $La_2Ce_2O_7$ and $LaNiO_3$ mixed oxides (5 wt% Ni). The best catalyst in this study was synthesized *via* hydrothermal synthesis and the boosted performance at both 600 and 850 °C was ascribed to the high number of oxygen vacancies in the $La_2Ce_2O_7$ support, with methane absorption and dissociation taking place on metallic Ni particles as uncovered from *in situ* XAS. The favorable interaction between Ni and Ce sites, in turn, improved the migration of active oxygen species and the reaction with adsorbed hydrogen and CH_x, and thereby, the deactivation *via* coking was minimized (< 2wt% C).[20]

Methane oxidation also suffers from severe deactivation hurdles. Based on detailed XAS studies of a Pd/Al_2O_3 (2 wt%) catalyst with short reductive pulses (SRP), it was shown that periodic lean condition could be leveraged to maintain the catalyst active state preventing the complete oxidation to PdO even with a continuous water vapor feed. Consequently, SRP could be exploited to overcome the deactivation *via* thermal and hydrothermal aging of the catalyst. While steady-state XAS investigations suggested that CH_4 oxidation is performed over fully oxidized Pd, the SRP procedure induced the presence of partially reduced Pd species that was linked to improved catalytic performance by online mass spectrometry. Finally, it was possible to ascribe the high performance for CH_4 oxidation and improved stability due to SRP to the presence of amorphous PdO_x species, which were either in contact with or vicinal to metallic Pd.[21]

In general, detailed investigations of the deactivation behavior of catalysts can easily constitute a time-consuming task being limited by the available beamtime at a synchrotron facility. Such deactivation processes can take several hours or even days, which makes detailed studies difficult at a beamline. For this purpose, laboratory-based XAS studies are emerging as a promising alternative to such synchrotron-based studies.[3,22,23]

Time-resolved XAS has also shown its great potential for unlocking the structure of catalysts under transient conditions, allowing the mechanisms of catalytic processes on the atomic scale to be probed. For instance, automotive gas after-treatment catalysts for the abatement of CO, NO_x, and hydrocarbons from the exhaust stream, are especially designed to operate under transient conditions. Therefore, transient XAS experiments are particularly beneficial in this case for uncovering complex structure-activity relationships. To investigate the reason for the poor low-temperature performance of a commercial copper-based zeolite catalyst (Cu-SSZ-13) during selective catalytic reduction (SCR) of NO_x by ammonia, Cu K-edge XAS was measured with 2 Hz repetition rate during NH_3 cut-off experiments, schematically represented in Fig. 1c.[24] Experiments were performed at various temperatures to probe the evolution of Cu speciation inside the zeolite cages during the removal of ammonia (NH_3 off) from a model exhaust gas mixture (1000 ppm NO, 6 vol% O_2, 6 vol% H_2O, and 1000 ppm NH_3 in N_2) flowing over the catalyst, and the concentration of NO and NH_3 at the reactor outlet measured by online mass spectrometry. High concentrations of a Cu(I) amino complex stabilized at lower temperatures were surmised as the primary reason for the inhibition of NO conversion to N_2. This finding allowed the efficiency of the catalytic converter to be increased by decreasing ammonia concentration in the pulsed ammonia feed.

Transient experiments can also be employed to identify the short-lived intermediates of catalytic reactions almost invisible under steady-state conditions. This methodology was successfully applied for understanding the reaction mechanism of oxidative dehydrogenation (ODH) of ethanol catalyzed by titania- and ceria-supported vanadia (VO_x) species.[25,26] By measuring *operando* V and Ti K-edge and Ce L_3-edge XANES during periodic removal of oxygen from the ethanol-oxygen feed, V^{4+}, V^{3+}, Ce^{3+}, and Ti^{3+} intermediates were detected by applying multivariate curve resolution analysis (Fig. 1d) to the large time-series datasets. Quantitative correlation of the catalytic rates of acetaldehyde formation to the initial rates of formation of respective intermediates provided evidence that V^{4+} and Ce^{3+} intermediates are directly involved in the catalytic cycles. Moreover, by investigating the reversibility of the V^{5+}/ V^{4+} and Ce^{4+}/Ce^{3+} redox processes during periodic modulation of the gas atmosphere, it was possible to distinguish active V^{4+} and Ce^{3+} intermediates from spectator V^{4+} and Ce^{3+} species present on the catalyst surface but not involved in catalysis.

The sample environment capabilities for heterogeneous catalysis involve various *in situ* and *operando* cells, such as capillary and stainless steel plug-flow reactors[27] with X-ray transparent window materials such as Kapton, operating at 1–40 bar and 25–800 °C. These cells can be combined with various gas analysis methods, including mass spectrometry, gas chromatography and infrared spectroscopy. At SLS 2.0, *in situ* and *operando* XRD and total scattering methods will also become a part of the Debye beamline portfolio and will be integrated with the same catalytic infrastructure, including cells and gas analytics.

4. Examples from Electrochemistry

In recent years, *operando* XAS has developed into an invaluable structure-sensitive probe for electrocatalytic systems, which is mirrored by an increasing representation of the electrocatalytic research community at the SuperXAS beamline. The growing demand for electrochemical energy storage and conversion technologies, necessitated by the drive towards a closed carbon cycle, has led to a wide array of research topics benefiting from the ability of *operando* XAS to elucidate the structural motif and electronic state of catalytic active sites. For example, while the oxygen evolution reaction (OER) is key to developing highly efficient water-splitting catalysts, carbon dioxide reduction (CO2RR) offers routes towards high-value-added chemicals and energy vectors. To enable such studies, the design of a reliable spectro-electrochemical cell is fundamental with considerations of the X-ray window material for sufficient transmission, limiting X-ray signal attenuation by the electrolyte, using a three-electrode configuration for accurate potential control and alleviating the accumulation of gas bubbles on the electrode surfaces. The spectro-electrochemical cell for studies at low current densities developed by Binninger *et al.* widely used at the SuperXAS beamline, utilizes a small internal volume three-electrode configuration with continuous electrolyte flow to address the aforementioned challenges (Fig. 2a).[28]

Mitigating the effects of undesirable radiation damage is of paramount importance to conducting reliable experiments. Through the optimization of a large area passivated implanted planar silicon (PIPS) detector for quick-scanning fluorescence detected XAS, giving access to sub-second XAS on low-loaded electrodes,[29] Diklic *et al.* could demonstrate that under acidic OER working conditions, electrode degradation in the X-ray beam was responsible for Ir^{3+} formation, while minimizing the

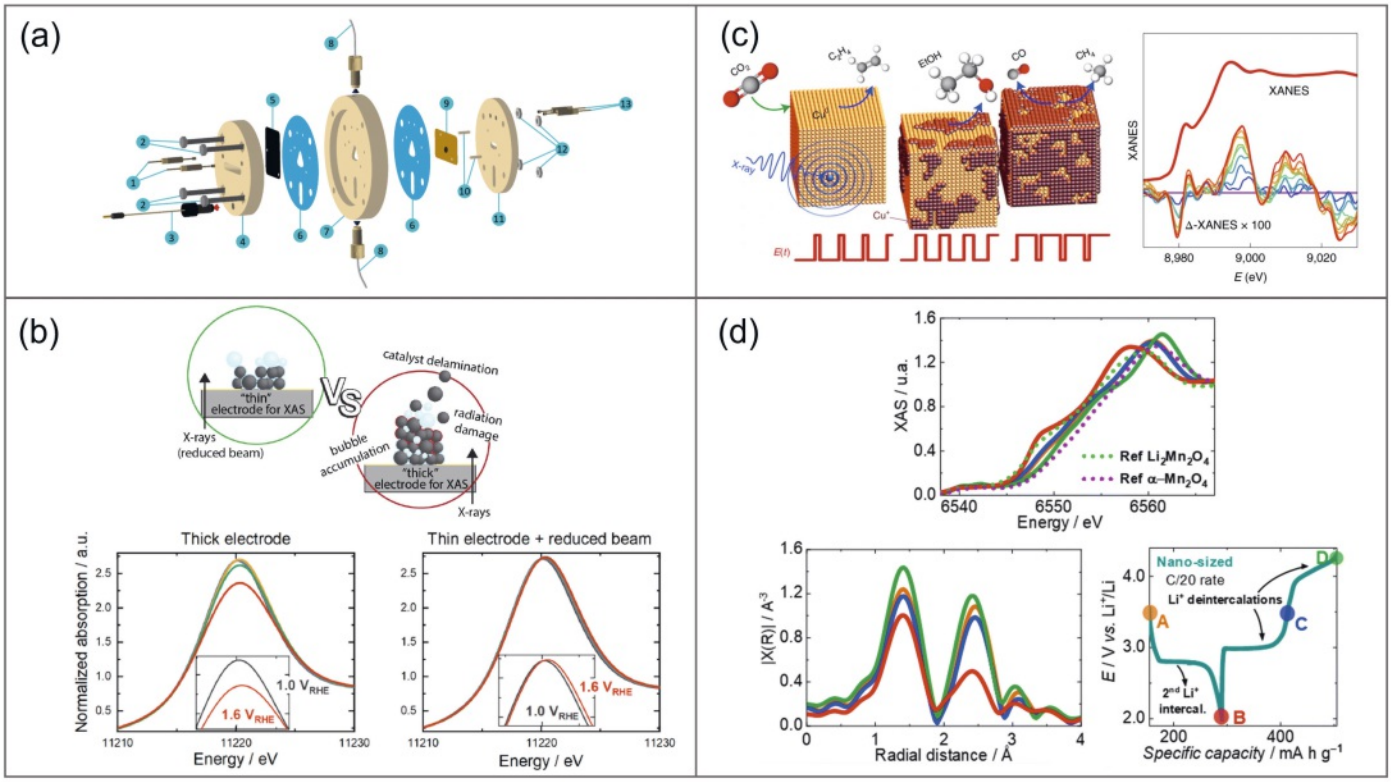

Fig. 2. a) Spectro-electrochemical flow cell design widely adopted for *operando* XAS studies at the SuperXAS beamline. Reproduced with permission from ref. [31] and used under CC BY 4.0 https://creativecommons.org/licenses/by/4.0/. b) Strategy for the mitigation of beam damage suffered in IrO_x electrodes during the oxygen evolution reaction performed in acid conditions whereby reducing electrode mass and X-ray beam flux gave reliable *in situ* XAS. Reproduced with permission from ref. [30] Copyright **2022** *American Chemical Society.* c) Effect of asymmetric pulse-voltammetry on the Cu catalyst surface structure and product selectivity for CO2RR together with exemplar XANES and differential data. Reproduced with permission from ref. [37] and used under CC BY 4.0 https://creativecommons.org/licenses/by/4.0. d) *Operando* charge-discharge cycling of a spinel-type $LiMn_2O_4$ cathode elucidating the reversible low voltage Jahn-Teller distortion in nanomaterials. Reproduced from ref. [38] with permission from *The Royal Society of Chemistry*.

working electrode thickness and decreasing the X-ray beam flux intensity lead to Ir^{5+} formation, (Fig. 2b), resolving the discrepancy on reported redox couples in the literature.[30] Thick electrodes, often necessitated for transmission XAS, significantly inhibit the collection of reliable experiments due to the negative impact on the electrochemistry being studied. Diercks *et al*. showed the importance of optimizing the electrode preparation for inhibiting mass transport limitations for reliable comparison of standard laboratory characterization and electrochemical performance, rather than optimizing for signal intensity for XAS.[31] More recently, the cell design of Binninger *et al*. has been adapted for shallow angle/grazing incidence measurements of highly dilute electrodes which, when coupled with quick fluorescence detection, opens up a new paradigm for highly time-resolved experiments to be performed on metal loadings even less than 50 μg/cm^2.[32]

Quick EXAFS (with sub-second time resolution), allows the electrochemical restructuring around elements of interest associated with the active site at the electrolyte-solid interface in *operando* by monitoring the working electrode current and product formation to be discerned. In the simplest case, exploring the active site formation can be resolved with short static potential holds. Kim *et al*. showed the structural transformation of $Ba_{0.5}Sr_{0.5}Co_{1-x}Fe_xO_{3-\delta}$ from edge-sharing to corner-sharing polyhedra, associated to the in-place formation of the OER Co-oxyhydroxide active surface. Such studies have illustrated how the characterization of materials under operation is critical to develop structure-function relationships for guiding the design of future OER materials.[33]

Fully utilizing the continuous developments at the SuperXAS beamline towards *operando* XAS for electrochemistry, cyclic voltammetry is the next exemplary case of taking standard laboratory characterization protocols and marrying them to *operando* XAS. Through the linear ramping of potential in both cathodic and anodic directions with time, Beall *et al*. could disentangle the importance of carbon additives to a perovskite electrode for alkaline OER demonstrating a fundamental involvement of carbon in enhancing the redox capacity of Co above acting solely to improve electrode conductivity.[34] Furthermore, periodic cycling enabled competing redox behaviors with progressing oxidation underlying a previously unobserved reversible phenomenon to be distinguished.

By exploiting the periodic nature of cyclic experimentation, highly time-resolved, or potential-resolved, insights can be gained with even challenging to measure low-loaded electrodes. Diklic *et al*. investigated a host of materials to illustrate that the formation of surface Ir^{5+} is a prerequisite for OER activity on Ir oxides. By using a sinusoidal potential stimulus, the saturation of the Ir oxide surface with Ir^{5+} was shown to universally precede the onset of OER.[35]

Applying a periodic stimulus is often referred to as modulation-excitation and can be used as a method to greatly improve the signal-to-noise ratio through utilizing phase-sensitive detection. In doing so, Ebner *et al*. investigated isolated Fe/N/C catalysts for the oxygen reduction reaction. Periodic squarewave potential modulation, otherwise referred to as pulse voltammetry, allowed the involvement of a distorted square-planar motif in the oxygen reduction reaction to be unraveled and the kinetic profiles of oxidation and reduction could be investigated.[36] Developing

further on this methodology, Timoshenko *et al*. employed asymmetric pulse voltammetry to influence the surface properties of a Cu-based catalyst for CO2RR by precisely tuning the asymmetry in the time at low and high potential.[37] Short high potential pulses favored stabilizing the metallic Cu surface and yielded high selectivity towards ethylene production. Sustained high potential operation led to substantial surface oxidation towards Cu^{2+} with CO2RR selectivity driven towards CH_4 and CO. Meanwhile, symmetric pulsed voltammetry XAS elucidated the stabilized formation of a defective surface oxide, which consequently steered the reaction towards the more valuable selective production of ethanol (Fig. 2c).

In the realm of energy materials, the ability to store and convert energy on demand is crucial. In the study of battery materials, understanding the local distortions that occur during operation is vital. For instance, during the discharge of lithium cathodes, the insertion of lithium into cubic spinels leads to a local axial distortion, making XAS the tool of choice for investigating such phenomena. To resolve the impact of lithiation on nano-size lithium manganese spinel, Falqueto *et al*. utilized *operando* XAS and reverse Monte Carlo EXAFS analyses to demonstrate that nano-spinels are amenable to the non-destructive formation of a Jahn-Teller distorted state (Fig. 2d). Taking this finding, a novel cycling protocol with periodic discharge was shown to not only recover charge capacity but aid in its increase, thereby mitigating charge capacity fading.[38]

5. Studies of Photo-induced Processes

The SuperXAS beamline also provides capabilities to study photo-induced changes of samples (including photo-catalysts) with a time resolution from a hundred picoseconds to hundreds of milliseconds (see Fig. 3a, d and g). This includes: i) pump-sequential-probes setup[39] that covers the time interval from 30 ns to 100 µs with an additional option to obtain one-time point with 100 ps resolution; (ii) pump-flow-probe setup[40] that operates in the time range from 100 µs to ~5 ms; and iii) setup for time-resolved fluorescence detection[41] with modulated light that is suitable for the 100 µs to 1s time range. In the pump-sequential-probes method a pulsed laser initiates the reaction and then information about the arrival time of each X-ray fluorescence photon coming from the sample is recorded with 20 ns precision. In the pump-flow-probe method the laser source excites the sample (containing for example a homogeneous photo-catalyst) in the liquid jet continuously. The spatial separation of laser and X-ray beams allows the control of the delay between the photoexcitation and probing. Time-resolved fluorescence detection has the same idea as the pump-sequential-probes method measuring the full kinetic information, but with a lower pre-defined resolution of 100 µs and typically using a modulated continuous light source (continuous wave laser or LED). Triggering of chemical reactions with pulsed lasers can be performed fast (within a nanosecond or faster) which opens the possibility to study short-lived catalytic

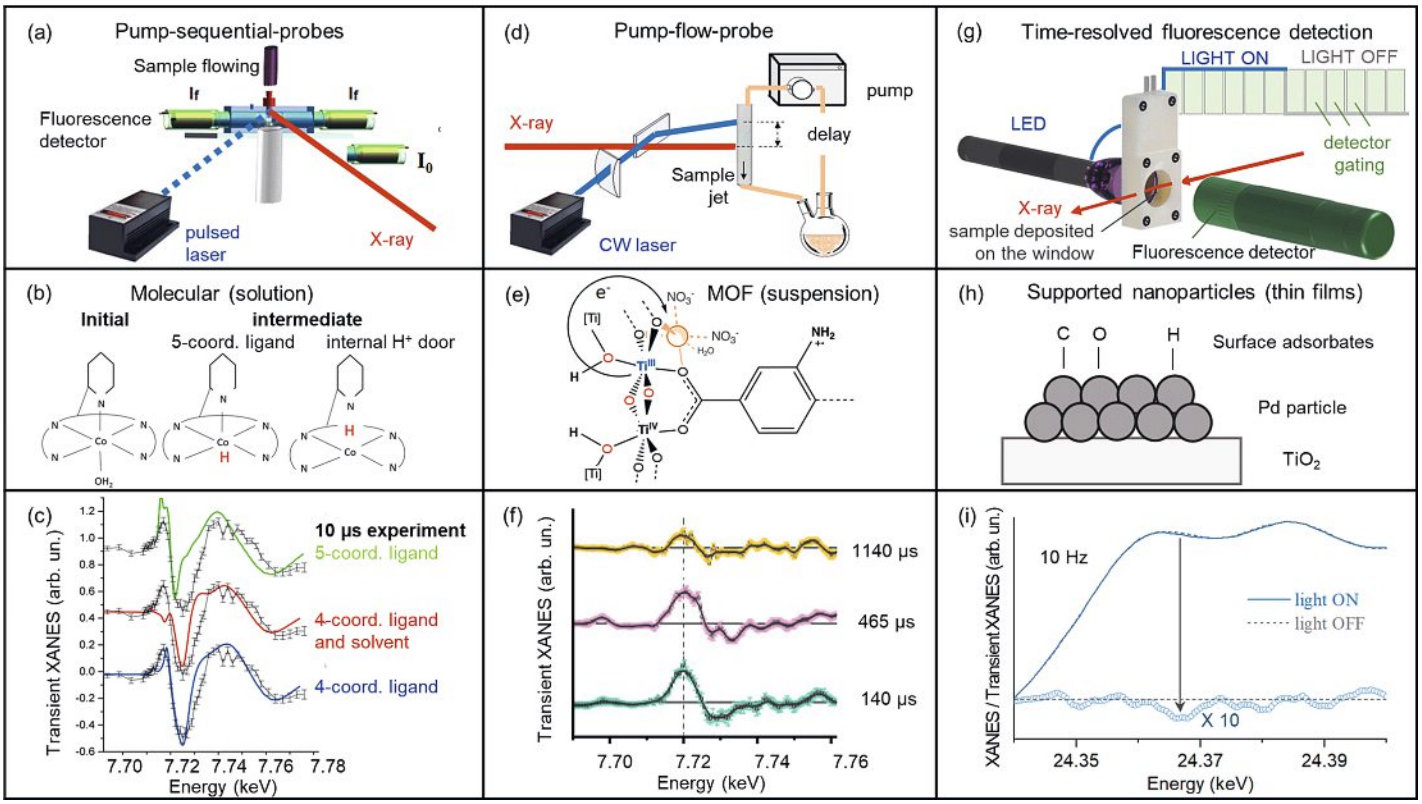

Fig. 3. a) Scheme of pump-sequential-probes XAS setup. b) Coordination environment of a Co center of a Co-polypyridyl hydrogen evolving catalyst in the initial state and for two alternative models of intermediate state with axial pyridinium acting as Co ligand or as intramolecular proton donor. c) Experimental Co K-edge transient XANES spectrum, corresponding to the 10 µs time window after photo-excitation (black lines), compared with theoretical calculations for models of the Co(I) with all 5 pyridyl groups coordinating Co (green line), with dissociation of axial pyridyl and vacant axial position (blue line) and with replacement of axial dissociated pyridyl by solvent molecule (red line). Adapted with permission from ref. [44]. Copyright **2018** *Wiley-VCH Verlag GmbH & Co. KGaA*, Weinheim. d) Scheme of pump-flow-probe XAS setup Adapted with permission from ref. [39], copyright **2013** *American Chemical Society*. e) Scheme of Co coordination and the electron transfer in Co@NH_2-MIL-125(Ti) metalloorganic framework. f) Experimental Co K-edge transient XANES spectrum of Co@NH_2-MIL-125(Ti) corresponding to different delays between photo-excitation and probing. Adapted with permission from ref. [48] and used under CC BY 4.0 https://creativecommons.org/licenses/by/4.0. g) Scheme of the setup for time-resolved fluorescence XAS detection and modulated light excitation. h) Schematic illustration of the potential surface adsorbates detectable by XANES. i) Pd K-edge XANES and difference XANES spectra collected with periodic 10 Hz UV light switching ON (blue) and OFF (grey), averaged over 6 h.

intermediates and with that photo-catalytic reaction mechanisms, including degradation pathways.

Molecular photocatalytic systems for solar energy conversion were in the focus of a series of investigations[42] at the SuperXAS beamline looking from the perspective of either the catalytic center[43,44] or the photosensitizer.[45,46] For example, in the photo-catalytic evolution of hydrogen from water, the first reaction step is the photo-induced electron transfer from the dye to the catalytic center with subsequent interaction with a proton. The structure of the first intermediate defines the whole reaction mechanism; the reaction can proceed either by intramolecular proton relay or alternatively by receiving protons directly from the solution. Such intermediates are expected to be present in the microsecond time range and were captured at the SuperXAS beamline using the pump-sequential-probe XAS technique.

The investigation of the Co(I) intermediate of a cobalt polypyridyl catalyst for hydrogen evolution (Fig. 3b) addressed the question of what the role of axial pyridyl is after the first electron transfer.[44] If it dissociates, it can potentially act as the intramolecular proton relay while if it remains bound to the Co center then the only available option is protonation from solution. Based on the comparison of the experimental Co K-edge transient XANES spectrum with theoretical calculations for different models of the Co(I) intermediate (Fig. 3c) it was found that the most realistic model includes the dissociation of axial pyridyl and the corresponding coordination site remains available for the protonation. The same method but with a slightly higher time resolution of ~30 ns can be used to investigate how the electronic and local atomic structure of photosensitizers changes after photo-excitation.[45,46] Rearrangements of local atomic structure are relevant because they typically lead to undesirable losses of energy received by absorbing the light and often facilitate faster decay of the system to the ground state, which reduces the quantum efficiency of the electron transfer to the catalyst.

Often photo-catalytic reactions proceed in multiple time ranges with short-lived intermediates formed within a microsecond but with the rate-limiting step taking many milliseconds. In such cases, the acquisition of time-resolved XAS spectra requires different experimental setups focusing either on the nanosecond-microsecond range (pump-sequential-probes method) or on the millisecond range (pump-flow-probe method or time-resolved fluorescence detection with modulated light source). To track short-lived intermediates efficiently, one must trigger the reaction at a rather high repetition rate on the order of 10 kHz, delivering a 'fresh' sample volume for each laser pulse. The sample volume is fresh if it was not excited by the laser during a few catalytic turnovers (for example during a few seconds before photo-excitation). This is readily achievable for samples in solution. Therefore, most pump-probe XAS experiments were performed for samples circulating in a flow system with a typical volume of ~40 mL forming an open jet at the point of interaction of the sample with X-rays and the laser. Since photo-excited photosensitizers can be often quenched by oxygen the open jet is enclosed in a chamber filled with nitrogen or helium.

To study slower processes, in the time range ranging from hundreds of microseconds to tens of milliseconds, the pump-flow-probe[40] method is used (Fig. 3d). The range of systems that can be studied is not limited to molecular systems in solution.[40–43] One of the possibilities is to use suspensions as was demonstrated for gold nanoparticles[47] and finely dispersed metalloorganic frameworks (MOFs)[48] using the pump-flow-probe method. In this recent study of NH_2-MIL-125(Ti) MOF loaded with Co the main question concerned the involvement of Co reduction as the photo-induced step (Fig. 3e) which can follow the initial formation of Ti^{III} sites produced due to the electron transfer from the MOF linker. The formation of Co(I) sites was confirmed by time-resolved XAS with long-lived reduced species observed already at ~100 μs and partially decaying at 1 ms time scale (Fig. 3f).[48] Thus photo-catalytic hydrogen evolution by NH_2-MIL-125(Ti) MOF loaded with cobalt occurs in parallel at Ti and Co with a long-lived reduced Co center acting as an efficient catalytic center. Hydrogen evolution at the Co center positively influences the stability of the MOF, which suffers from linker elimination from the framework when the reaction proceeds only at the Ti sites.

Photo-induced processes in the time range from 100 μs and slower can also be studied using time-resolved fluorescence detection. As an example, Fig. 3g shows an experimental setup to explore the structure of Pd-promoted TiO_2 catalyst during photo-catalytic hydrogen evolution. The catalytic ink was prepared by mixing 2% Pd/TiO_2 with methanol and was then deposited on the window of the photo-catalytic cell. After the applied catalyst was completely dried, the cell was filled with water and methanol as a hole scavenger.[49] The UV LED was positioned from the back side of the cell and was switched ON and OFF periodically with a frequency of 1-10 Hz. The fluorescence signal was recorded with a 100 times higher frequency than the UV switching. For Pd K-edge XANES of small (2-3 nm) palladium particles, bonding with C, O or H atoms (Fig. 3h) can be detected in both bulk and surface regions.[50–52] The collected data with 10 Hz UV switching frequency (Fig. 3i) indicated the presence of Pd(0) species with a small difference in the shape of XANES around the first peak at 24.366 keV, similar to that observed for Pd–C bonding.

6. *Operando* X-ray Emission Spectroscopy

Throughout the operation of the SuperXAS beamline at SLS, XES has undergone continuous evolution with the development of cutting-edge spectrometers and experimental methodologies.

In more recent years, the von Hamos geometry spectrometer has developed into the preferred mode for time-resolved XES.[53] With the implementation of the von Hamos spectrometer high energy resolution off-resonant spectroscopy was developed and allowed to monitor the *in situ* decomposition of $Pt(acac)_2$ in hydrogen revealing the presence of a partially reduced intermediate.[54] The von Hamos geometry was also employed for non-resonant XES at the S K_α emission line and proved to be a powerful tool in evaluating the speciation of ppm levels of sulphur.[55] Non-resonant XES allowed moderate time resolution to be achieved to investigate *operando* mechanism of sulphur poisoning and regeneration of Ru/SiO_2 and Ru/Al_2O_3 methanation catalysts in the presence of H_2S.[56]

Non-resonant XES can also be used to enable time-resolved studies at the K_β emission lines. For example, with the *in situ* investigation of Fe/N/C electrocatalysts Saveleva *et al.* were able to establish unambiguously the potential-induced spin state change of Fe. This provided novel insights into the changes in Fe electron density distribution aiding the understanding of the catalytic mechanisms.[57] Leveraging on the increased flux yielded by employing a multilayer monochromator for broadband or with pink beam operation (which has high energy cut-off defined by the collimating X-ray mirror), time resolved core-to-core XES measurements of sub-mM concentrations samples are possible giving spin state sensitivity. [58]

Finally, the development of a DuMond-type crystal spectrometer enables high energy XES in the range of 15-26 keV to be reached, which gives access to the measurement of $K_{\beta 2}$ lines of 4d elements with resolution sufficient to observe the chemical environment of the 4d transition metal of interest.[59]

As part of the SLS 2.0 upgrade project, a new X-ray emission spectrometer with ~10 times higher collection efficiency is under development. In combination with broadband and pink-beam operation modes, that provide 2–3 orders of magnitude higher incident X-ray flux, a significant improvement of statistics for non-resonant X-ray emission spectroscopy is expected. This

further opens possibilities for time-resolved X-ray emission measurements, which give complementary information about the spin and oxidation state of transition metals compared to XAS, as well as specific details about metal ligands, for example, their protonation.[60,61]

7. Conclusions and Outlook

Synchrotron-based X-ray absorption and emission spectroscopy are powerful tools that allow insights into the electronic and local geometric structures of the elements of interest under *operando* conditions.

Through reviewing recent examples from heterogeneous catalysis, electrochemistry, and photochemistry, we have shown the capabilities of the SuperXAS beamline at the SLS for obtaining structure-performance relationships. These capabilities include world-leading sub-second time resolution attained by quick XAS and broadband non-resonant XES, which allow the combination of *operando* studies with transient experimentation. Such studies help to uncover active sites distinguishing them from spectators or to determine the rate-limiting step of catalytic processes. Even higher time resolution is obtained with laser pump–X-ray probe spectroscopy, which allows insight in the mechanisms of photo-induced processes to be obtained.

When SLS 2.0 becomes available for user experiments (mid-2025), capabilities for hard X-ray spectroscopy will be doubled by the addition of the new Debye beamline to the SLS portfolio, which will allow for quasi-simultaneous quick XAS and powder diffraction. Dedicated gas infrastructure will enable work with pressures of up to 60 bar for most reactive gases. Furthermore, by providing access to gas analytics (GC, MS, FTIR), potentiostats, *operando* cells, and support with data analysis, we hope to further facilitate the transition of complex experiments from laboratory to our beamlines to help answer important scientific questions.

Acknowledgements

We would like to thank all current and previous group members of the *operando* spectroscopy group for their contributions to the development of the SuperXAS beamline and for pushing forward some of the research presented here. This publication was created as part of NCCR Catalysis (grant number 180544), a National Centre of Competence in Research funded by the Swiss National Science Foundation.

Received: March 25. 2024

[1] S. Calvin, 'XAFS for Everyone', CRC Press, Boca Raton, **2013**, https://doi.org/10.1201/b14843.
[2] O. Müller, M. Nachtegaal, J. Just, D. Lützenkirchen-Hecht, R. Frahm, *J. Synchrotron Radiat*. **2016**, *23*, 260, https://doi.org/10.1107/S1600577515018007.
[3] N. S. Genz, A. J. Kallio, R. Oord, F. Krumeich, A. Pokle, Ø. Prytz, U. Olsbye, F. Meirer, S. Huotari, B. M. Weckhuysen, *Angew. Chem. Int. Ed*. **2022**, *61*, e202209334, https://doi.org/10.1002/anie.202209334.
[4] W. Błachucki, J. Czapla-Masztafiak, J. Sá, J. Szlachetko, *J. Anal. At. Spectrom*. **2019**, *34*, 1409, https://doi.org/10.1039/c9ja00159j.
[5] P. M. Abdala, O. V. Safonova, G. Wiker, W. Van Beek, H. Emerich, J. A. V. Bokhoven, J. Sá, J. Szlachetko, M. Nachtegaal, *CHIMIA* **2012**, *66*, 699, https://doi.org/10.2533/chimia.2012.699.
[6] T. N. Ansari, R. H. Choudhary, M. Nachtegaal, A. H. Clark, S. V Plummer, J. B. Jasinki, F. Gallou, S. Handa, *ACS Catal*. **2024**, *14*, 4099, https://doi.org/10.1021/acscatal.3c06351.
[7] S. Büchele, A. Yakimov, S. M. Collins, A. Ruiz-Ferrando, Z. Chen, E. Willinger, D. M. Kepaptsoglou, Q. M. Ramasse, C. R. Müller, O. V. Safonova, N. López, C. Copéret, J. Pérez-Ramírez, S. Mitchell, *Small* **2022**, *18*, https://doi.org/10.1002/smll.202202080.
[8] S. K. Kaiser, E. Fako, I. Surin, F. Krumeich, V. A. Kondratenko, E. V Kondratenko, A. H. Clark, N. López, J. Pérez-Ramírez, *Nat. Nanotechnol*. **2022**, *17*, 606, https://doi.org/10.1038/s41565-022-01105-4.
[9] J. B. Falqueto, A. H. Clark, A. Štefančič, G. J. Smales, C. A. F. Vaz, A. J. Schuler, N. Bocchi, M. El Kazzi, *ACS Appl. Energy Mater.* **2022**, *5*, 8357, https://doi.org/10.1021/acsaem.2c00902.
[10] V. V Nenonen, R. Kaegi, S. J. Hug, J. Göttlicher, S. Mangold, L. H. E. Winkel, A. Voegelin, *Geochim. Cosmochim. Acta* **2023**, *360*, 207, https://doi.org/10.1016/j.gca.2023.09.004.
[11] M. Paulikat, D. Vitone, F. K. Schackert, N. Schuth, A. Barbanente, G. M. Piccini, E. Ippoliti, G. Rossetti, A. H. Clark, M. Nachtegaal, M. Haumann, H. Dau, P. Carloni, S. Geremia, R. De Zorzi, L. Quintanar, F. Arnesano, *J. Chem. Inf. Model.* **2023**, *63*, 161, https://doi.org/10.1021/acs.jcim.2c01164.
[12] J. Singh, E. M. C. Alayon, M. Tromp, O. V. Safonova, P. Glatzel, M. Nachtegaal, R. Frahm, J. A. Van Bokhoven, *Angew. Chem. Int. Ed.* **2008**, *47*, 9260, https://doi.org/10.1002/anie.200803427.
[13] L. Rochlitz, J. W. A. Fischer, Q. Pessemesse, A. H. Clark, A. Ashuiev, D. Klose, P. A. Payard, G. Jeschke, C. Copéret, *JACS Au* **2023**, *3*, 1939, https://doi.org/10.1021/jacsau.3c00197.
[14] V. Giulimondi, A. Ruiz-Ferrando, G. Giannakakis, I. Surin, M. Agrachev, G. Jeschke, F. Krumeich, N. López, A. H. Clark, J. Pérez-Ramírez, *Nat. Commun*. **2023**, *14*, 1, https://doi.org/10.1038/s41467-023-41344-0.
[15] J. L. Alfke, A. Müller, A. H. Clark, A. Cervellino, M. Plodinec, A. Comas-Vives, C. Copéret, O. V. Safonova, *Phys. Chem. Chem. Phys.* **2022**, *24*, 24429, https://doi.org/10.1039/d2cp03593f.
[16] T. Fovanna, M. Nachtegaal, A. H. Clark, O. Kröcher, D. Ferri, *ACS Catal.* **2023**, *13*, 3323, https://doi.org/10.1021/acscatal.2c04791.
[17] T. Fovanna, I. Alxneit, A. H. Clark, S. Checchia, M. Di Michiel, O. Kröcher, M. Nachtegaal, D. Ferri, *J. Phys. Chem. C* **2021**, *125*, 16473, https://doi.org/10.1021/acs.jpcc.1c01882.
[18] I. I. Sadykov, M. Zabilskiy, A. H. Clark, F. Krumeich, V. Sushkevich, J. A. van Bokhoven, M. Nachtegaal, O. V. Safonova, *ACS Catal*. **2021**, *11*, 11793, https://doi.org/10.1021/acscatal.1c02795.
[19] I. I. Sadykov, V. L. Sushkevich, F. Krumeich, R. J. G. Nuguid, J. A. van Bokhoven, M. Nachtegaal, O. V. Safonova, *Angew. Chem. Int. Ed*. **2023**, *62*, e202214032, https://doi.org/10.1002/anie.202214032.
[20] A. P. Ramon, X. Li, A. H. Clark, O. V. Safonova, F. C. Marcos, E. M. Assaf, J. A. van Bokhoven, L. Artiglia, J. M. Assaf, *Appl. Catal. B Environ*. **2022**, *315*, 121528, https://doi.org/10.1016/j.apcatb.2022.121528.
[21] T. Franken, M. Roger, A. W. Petrov, A. H. Clark, M. Agote-Arán, F. Krumeich, O. Kröcher, D. Ferri, *ACS Catal*. **2021**, *11*, 4870, https://doi.org/10.1021/acscatal.1c00328.
[22] N. S. Genz, A.-J. Kallio, F. Meirer, S. Huotari, B. M. Weckhuysen, *Chemistry–Methods* **2024**, *4*, e202300027, https://doi.org/10.1002/cmtd.202300027.
[23] J. G. Moya-Cancino, A. P. Honkanen, A. M. J. van der Eerden, H. Schaink, L. Folkertsma, M. Ghiasi, A. Longo, F. Meirer, F. M. F. de Groot, S. Huotari, B. M. Weckhuysen, *ChemCatChem* **2019**, *11*, 3042, https://doi.org/10.1002/cctc.201900434.
[24] A. Marberger, A. W. Petrov, P. Steiger, M. Elsener, O. Kröcher, M. Nachtegaal, D. Ferri, *Nat. Catal.* **2018**, *1*, 221, https://doi.org/10.1038/s41929-018-0032-6.
[25] A. Zabilska, M. Zabilskiy, R. J. G. Nuguid, A. H. Clark, I. I. Sadykov, M. Nachtegaal, O. Kröcher, O. V. Safonova, *Angew. Chem. Int. Ed*. **2023**, *62*, e202301297, https://doi.org/10.1002/anie.202301297.
[26] A. Zabilska, A. H. Clark, B. M. Moskowitz, I. E. Wachs, Y. Kakiuchi, C. Copéret, M. Nachtegaal, O. Kröcher, O. V. Safonova, *JACS Au* **2022**, *2*, 762, https://doi.org/10.1021/jacsau.2c00027.
[27] G. L. Chiarello, M. Nachtegaal, V. Marchionni, L. Quaroni, D. Ferri, *Rev. Sci. Instrum*. **2014**, *85*, 74102, https://doi.org/10.1063/1.4890668.
[28] T. Binninger, E. Fabbri, A. Patru, M. Garganourakis, J. Han, D. F. Abbott, O. Sereda, R. Kötz, A. Menzel, M. Nachtegaal, T. J. Schmidt, *J. Electrochem. Soc*. **2016**, *163*, H906, https://doi.org/10.1149/2.0201610jes.
[29] A. H. Clark, P. Steiger, B. Bornmann, S. Hitz, R. Frahm, D. Ferri, M. Nachtegaal, *J. Synchrotron Radiat*. **2020**, *27*, 681, https://doi.org/10.1107/S1600577520002350.
[30] N. Diklić, A. H. Clark, J. Herranz, J. S. Diercks, D. Aegerter, M. Nachtegaal, A. Beard, T. J. Schmidt, *ACS Energy Let*. **2022**, *7*, 5, 1735, https://doi.org/10.1021/acsenergylett.2c00727.
[31] J. S. Diercks, J. Herranz, K. Ebner, N. Diklić, M. Georgi, P. Chauhan, A. H. Clark, M. Nachtegaal, A. Eychmüller, T. J. Schmidt, *Angew. Chem. Int. Ed*. **2023**, *62*, https://doi.org/10.1002/anie.202216633.
[32] M. Winzely, J. S. Diercks, O. V. Safonova, P. Rüttimann, A. H. Clark, P. M. Leidinger, S. Phadke, M. Nachtegaal, T. J. Schmidt, J. Herranz, in '244th ECS Meeting (October 8-12, 2023)', ECS, **2023**.
[33] B. J. Kim, E. Fabbri, D. F. Abbott, X. Cheng, A. H. Clark, M. Nachtegaal, M. Borlaf, I. E. Castelli, T. Graule, T. J. Schmidt, *J. Am. Chem. Soc.* **2019**, *141*, 5231, https://doi.org/10.1021/jacs.8b12101.
[34] C. E. Beall, E. Fabbri, A. H. Clark, N. S. Yüzbasi, T. Graule, T. J. Schmidt, *EcoMat* **2023**, *5*, e12353, https://doi.org/10.1002/eom2.12353.
[35] N. Diklić, A. H. Clark, J. Herranz, D. Aegerter, J. S. Diercks, A. Beard, V. A. Saveleva, P. Chauhan, M. Nachtegaal, T. Huthwelker, D. Lebedev, P. Kayser, J. A. Alonso, C. Copéret, T. J. Schmidt, *ACS Catal*. **2023**, *13*, 11069, https://doi.org/10.1021/acscatal.3c01448.
[36] K. Ebner, A. H. Clark, V. A. Saveleva, G. Smolentsev, J. Chen, L. Ni, J. Li, A. Zitolo, F. Jaouen, U. I. Kramm, T. J. Schmidt, J. Herranz, *Adv. Energy Mater*. **2022**, *12*, 2103699, https://doi.org/10.1002/AENM.202103699.

[37] J. Timoshenko, A. Bergmann, C. Rettenmaier, A. Herzog, R. M. Arán-Ais, H. S. Jeon, F. T. Haase, U. Hejral, P. Grosse, S. Kühl, E. M. Davis, J. Tian, O. Magnussen, B. Roldan Cuenya, *Nat. Catal*. **2022**, *5*, 259, https://doi.org/10.1038/s41929-022-00760-z.
[38] J. B. Falqueto, A. H. Clark, Ł. Kondracki, N. Bocchi, M. El Kazzi, *J. Mater. Chem. A* **2023**, *11*, 24800, https://doi.org/10.1039/d3ta04660e.
[39] G. Smolentsev, A. A. Guda, M. Janousch, C. Frieh, G. Jud, F. Zamponi, M. Chavarot-Kerlidou, V. Artero, J. A. Van Bokhoven, M. Nachtegaal, *Fara. Discuss*. **2014**, *171*, 259, https://doi.org/10.1039/c4fd00035h.
[40] G. Smolentsev, A. Guda, X. Zhang, K. Haldrup, E. S. Andreiadis, M. Chavarot-Kerlidou, S. E. Canton, M. Nachtegaal, V. Artero, V. Sundstrom, *J. Phys. Chem. C* **2013**, *117*, 17367, https://doi.org/10.1021/jp4010554.
[41] A. A. Guda, A. L. Bugaev, R. Kopelent, L. Braglia, A. V. Soldatov, M. Nachtegaal, O. V. Safonova, G. Smolentsev, *J. Synchrotron Radiat.* **2018**, *25*, 989, https://doi.org/10.1107/S1600577518005325.
[42] G. Smolentsev, V. Sundström, *Coord. Chem. Rev*., **2015**, *304*, 117, https://doi.org/10.1016/j.ccr.2015.03.001.
[43] G. Smolentsev, B. Cecconi, A. Guda, M. Chavarot-Kerlidou, J. A. Van Bokhoven, M. Nachtegaal, V. Artero, *Chem. Eur. J.* **2015**, *21*, 15158, https://doi.org/10.1002/chem.201502900.
[44] G. Smolentsev, M. A. Soldatov, B. Probst, C. Bachmann, N. Azzaroli, R. Alberto, M. Nachtegaal, J. A. van Bokhoven, *ChemSusChem* **2018**, *11*, 3087, https://doi.org/10.1002/cssc.201801140.
[45] A. Guda, J. Windisch, B. Probst, J. A. Van Bokhoven, R. Alberto, M. Nachtegaal, L. X. Chen, G. Smolentsev, *Phys. Chem. Chem. Phys.* **2021**, *23*, 26729, https://doi.org/10.1039/d1cp02823e.
[46] G. Smolentsev, K. M. Van Vliet, N. Azzaroli, J. A. Van Bokhoven, A. M. Brouwer, B. De Bruin, M. Nachtegaal, M. Tromp, *Photochem. Photobiol. Sci*. **2018**, *17*, 896, https://doi.org/10.1039/c8pp00065d.
[47] F. Zamponi, T. J. Penfold, M. Nachtegaal, A. Lübcke, J. Rittmann, C. J. Milne, M. Chergui, J. A. van Bokhoven, *Phys. Chem. Chem. Phys.* **2014**, *16*, 23157, https://doi.org/10.1039/c4cp03301a.
[48] V. Kavun, E. Uslamin, B. van der Linden, S. Canossa, A. Goryachev, E. E. Bos, J. Garcia Santaclara, G. Smolentsev, E. Repo, M. A. van der Veen, *ACS Appl. Mater. Interfaces* **2023**, *15*, 54601, https://doi.org/10.1021/acsami.3c15490.
[49] E. G. Kozyr, P. N. Njoroge, S. V. Chapek, V. V. Shapovalov, A. A. Skorynina, A. Y. Pnevskaya, A. N. Bulgakov, A. V. Soldatov, F. Pellegrino, E. Groppo, S. Bordiga, L. Mino, A. L. Bugaev, *Catalysts* **2023**, *13*, 414, https://doi.org/10.3390/catal13020414.
[50] A. L. Bugaev, M. Zabilskiy, A. A. Skorynina, O. A. Usoltsev, A. V. Soldatov, J. A. Van Bokhoven, *Chem. Commun*. **2020**, *56*, 13097, https://doi.org/10.1039/d0cc05050d.
[51] M. W. Tew, M. Nachtegaal, M. Janousch, T. Huthwelker, J. A. Van Bokhoven, *Phys. Chem. Chem. Phys*. **2012**, *14*, 5761, https://doi.org/10.1039/c2cp24068h.
[52] A. L. Bugaev, A. A. Guda, A. Lazzarini, K. A. Lomachenko, E. Groppo, R. Pellegrini, A. Piovano, H. Emerich, A. V. Soldatov, L. A. Bugaev, V. P. Dmitriev, J. A. van Bokhoven, C. Lamberti, *Catal. Today* **2017**, *283*, 119, https://doi.org/10.1016/j.cattod.2016.02.065.
[53] J. Szlachetko, M. Nachtegaal, E. De Boni, M. Willimann, O. Safonova, J. Sa, G. Smolentsev, M. Szlachetko, J. A. Van Bokhoven, J. C. Dousse, J. Hoszowska, Y. Kayser, P. Jagodzinski, A. Bergamaschi, B. Schmitt, C. David, A. Lücke, 'Review of Scientific Instruments', Vol. 83, AIP Publishing, **2012**, p. 103105, https://doi.org/10.1063/1.4756691.
[54] J. Szlachetko, M. Nachtegaal, J. Sá, J. C. Dousse, J. Hoszowska, E. Kleymenov, M. Janousch, O. V Safonova, C. König, J. A. Van Bokhoven, *Chem. Commun*. **2012**, *48*, 10898, https://doi.org/10.1039/c2cc35086f.
[55] D. Kuzmenko, U. Vogelsang, S. Hitz, D. Müller, A. H. Clark, D. Kinschel, J. Czapla-Masztafiak, C. Milne, J. Szlachetko, M. Nachtegaal, *J. Anal. At. Spectrom*. **2019**, *34*, 2105, https://doi.org/10.1039/c9ja00195f.
[56] D. Kuzmenko, A. H. Clark, T. Schildhauer, J. Szlachetko, M. Nachtegaal, *RSC Adv.* **2020**, *10*, 15853, https://doi.org/10.1039/d0ra03068f.
[57] V. A. Saveleva, K. Ebner, L. Ni, G. Smolentsev, D. Klose, A. Zitolo, E. Marelli, J. Li, M. Medarde, O. V Safonova, M. Nachtegaal, F. Jaouen, U. I. Kramm, T. J. Schmidt, J. Herranz, *Angew. Chem. Int. Ed*. **2021**, *60*, 11707, https://doi.org/10.1002/anie.202016951.
[58] O. Dikaya, M. Nachtegaal, J. Szlachetko, K. Ebner, V. Saveleva, N. Weder, B. Probst, R. Alberto, D. Serebrennikov, E. Clementyev, K. Maksimova, A. Goikhman, G. Smolentsev, *Results Phys.* **2020**, *18*, https://doi.org/10.1016/j.rinp.2020.103212.
[59] P. Jagodziński, J. Szlachetko, J. C. Dousse, J. Hoszowska, M. Szlachetko, U. Vogelsang, D. Banaś, T. Pakendorf, A. Meents, J. A. Van Bokhoven, A. Kubala-Kukuś, M. Pajek, M. Nachtegaal, *Rev. Sci. Instrum*. **2019**, *90*, 63106, https://doi.org/10.1063/1.5087948.
[60] P. Glatzel, G. Smolentsev, G. Bunker, *J. Phys.: Conf. Ser.* **2009**, *190*, https://doi.org/10.1088/1742-6596/190/1/012046.
[61] G. Smolentsev, A. V Soldatov, J. Messinger, K. Merz, T. Weyhermüller, U. Bergmann, Y. Pushkar, J. Yano, V. K. Yachandra, P. Glatzel, *J. Am. Chem. Soc*. **2009**, *131*, 13161, https://doi.org/10.1021/ja808526m.

License and Terms

The definitive version of this article is the electronic one that can be found at https://doi.org/10.2533/chimia.2024.304